

THE COMPLEX ZEROS OF RANDOM SUMS

BY ROBERT J. VANDERBEI*

Princeton University

This paper is dedicated to the memory of Larry Shepp.

This paper extends earlier work on the distribution in the complex plane of the roots of random polynomials. In this paper, the random polynomials are generalized to random finite sums of given “basis” functions. The basis functions are assumed to be entire functions that are real-valued on the real line. The coefficients are assumed to be independent identically distributed Normal $(0, 1)$ random variables. An explicit formula for the density function is given in terms of the set of basis functions. We also consider some practical examples including Fourier series. In some cases, we derive an explicit formula for the limiting density as the number of terms in the sum tends to infinity.

1. Introduction.. The problem of characterizing the distribution of the roots of random polynomials has a long history. In 1943, Kac [15] studied the real roots of random polynomials with iid normal coefficients. He obtained an explicit formula for the density function for the distribution of the real roots.

Following the initial work of Kac, a large body of research on zeros of random polynomials has appeared – see [2] for a fairly complete account of the early work in this area including an extensive list of references. Most of this early work focused on the real zeros; [5], [8] and [25] being a few notable exceptions. The paper of Edelman and Kostlan [4] gives a very elegant geometric treatment of the problem.

In more recent years, the work has branched off in a number of directions. For example, in 1995, Larry Shepp and I derived an explicit formula for the distribution of the roots in the complex plane (see [22]) when the coefficients are assumed to be iid normal random variables. A short time later, Ibragimov and Zeitouni [11] took a different approach and were able to rederive our results and also find limiting distributions as the degree n tends to infinity

*Research supported by ONR through grant N00014-13-1-0093 and N00014-16-1-2162
Primary 30C15; secondary 30B20, 26C10, 60B99

under more general distributional assumptions. See also [13] and [14].

Also in the late 1990's, it was pointed out that understanding deeper statistical properties of the random roots, such as k -point correlations among the roots, was both interesting mathematically and had important implications in physics (see, e.g., [20], [7] and [21]).

A number of papers have appeared that attempt to prove certain specific properties under increasingly general distributional assumptions. For example, in 2002, Dembo et al. [3] derived a formula for the probability that none of the roots are real (assuming n is even, of course) in the case when the coefficients of the polynomial are iid but not necessarily normal. Other papers have continued to study real roots—see, e.g., [12]. Another property that has been actively studied in recent years is the fact that as n gets large the complex roots tend to distribute themselves close to and uniformly about the unit circle in the complex planes—see, e.g., the papers by Shiffman and Zelditch [23], Hughes and Nikeghbali [9], Ibragimov and Zaporozhets [10], Pritsker and Yeager [19] and Pritsker [18]. Also, Li and Wei [17] have considered harmonic polynomials—polynomials in the complex variable z and its conjugate \bar{z} .

Using a very different approach, Feldheim [6] has derived a result that with some work can be shown to be equivalent to the results presented herein.

Recently, Tao and Vu [24], drawing on the close connection with random matrix theory, derived asymptotic formulas for the correlation functions of the roots of random polynomials. They specifically address the question of how many zeros are real.

The results summarized above mostly establish certain properties of the roots under very general distributional assumptions. The price paid for that generality is that most results only hold asymptotically as $n \rightarrow \infty$. In contrast, this paper introduces a modest generalization to the core assumptions underlying the results in [22] and we show that analogous explicit formulas can still be derived for any value of n . Specifically, instead of considering polynomials, $\sum_{j=0}^n \eta_j z^j$, we generalize the “basis” functions z^j to be any set of entire functions, $f_j(z)$, that are real on the real line. So, to that end, we let

$$P_n(z) = \sum_{j=0}^n \eta_j f_j(z), \quad z \in \mathbf{C},$$

where n is a fixed integer, the η_j 's are independent identically distributed $N(0, 1)$ random variables, and the functions f_j are given entire functions that are real-valued on the real line. We derive an explicit formula for the expected number of zeros in any measurable subset Ω of the complex plane

C. The formula will be expressed in terms of the following functions:

$$\begin{aligned} A_0(z) &= \sum_{j=0}^n f_j(z)^2, & B_0(z) &= \sum_{j=0}^n |f_j(z)|^2, \\ A_1(z) &= \sum_{j=0}^n f_j(z)f'_j(z), & B_1(z) &= \sum_{j=0}^n \overline{f_j(z)}f'_j(z), \\ A_2(z) &= \sum_{j=0}^n f'_j(z)^2, & B_2(z) &= \sum_{j=0}^n |f'_j(z)|^2, \end{aligned}$$

and

$$(1) \quad D_0(z) = \sqrt{B_0(z)^2 - |A_0(z)|^2}.$$

and, lastly,

$$E_1(z) = \sqrt{A_2(z)A_0(z) - A_1(z)^2}.$$

Notes: (1) As usual, an overbar denotes complex conjugation and primes denote differentiation with respect to z . (2) The function E_1 will only be needed in places where the argument of the square root is a positive real. At such places, the square root is assumed to be a positive real. (3) Throughout the paper, we follow the usual convention of denoting the real and imaginary parts of a complex variable z by x and y , respectively, i.e., $z = x + iy$.

Let $\nu_n(\Omega)$ denote the (random) number of zeros of P_n in a set Ω in the complex plane. Our first theorem asserts that throughout most of the plane this random variable has a density with respect to Lebesgue measure on the plane:

THEOREM 1.1. *For each measurable set $\Omega \subset \{z \in \mathbf{C} \mid D_0(z) \neq 0\}$,*

$$(2) \quad \mathbf{E}\nu_n(\Omega) = \int_{\Omega} h_n(x, y) dx dy,$$

where

$$h_n(z) = \frac{B_2 D_0^2 - B_0(|B_1|^2 + |A_1|^2) + (A_0 B_1 \overline{A_1} + \overline{A_0} \overline{B_1} A_1)}{\pi D_0^3}.$$

It is easy to see that the density function h_n is real valued. It is less obvious that it is nonnegative. We leave this sanity check to the reader. As we see from the above theorem, places where D_0 vanishes are special and must be studied separately. The real axis is one such place:

THEOREM 1.2. *On the real line, the function D_0 vanishes. For each measurable set $\Omega \subset \mathbb{R}$,*

$$(3) \quad \mathbf{E}\nu_n(\Omega) = \int_{\Omega} g_n(x) dx,$$

where

$$g_n(x) = \frac{E_1(x)}{\pi B_0}.$$

In the case where the $f_j(z)$'s are just powers of z , our results reduce to those given in [22]. The proof here parallels the analogous proof given in [22] but there are a few differences, the most important one being the fact that, in general, the function B_1 is not real-valued like it was in [22]. It seems that this explicit formula has not been derived before and, as shown in later sections, there are interesting new examples that can now be solved.

While the definition of h_n in Theorem 1.1 looks rather complicated, it is nevertheless amenable both to computation and, with some choices of the functions f_j , it is amenable to asymptotic analysis as well.

In the following section, we derive the explicit formulas given above for the intensity functions h_n and g_n . Then, in Section 3, we look at some specific examples and finally, in Section 4, we offer some speculation and suggest future research directions.

2. The Intensity Functions h_n and g_n . This section is devoted to the proof of Theorems 1.1 and 1.2. We begin with the following proposition.

PROPOSITION 2.1. *For each region $\Omega \in \mathbb{C}$ whose boundary intersects the set $\{z \mid D_0(z) = 0\}$ at most only finitely many times,*

$$(4) \quad \mathbf{E}\nu_n(\Omega) = \frac{1}{2\pi i} \int_{\partial\Omega} F(z) dz,$$

where

$$(5) \quad F = \frac{B_1 D_0 + B_0 B_1 - \bar{A}_0 A_1}{B_0 D_0 + B_0^2 - \bar{A}_0 A_0}.$$

PROOF. The argument principle (see, e.g., [1], p. 151) gives an explicit formula for the random variable $\nu_n(\Omega)$, namely

$$(6) \quad \nu_n(\Omega) = \frac{1}{2\pi i} \int_{\partial\Omega} \frac{P'_n(z)}{P_n(z)} dz.$$

Taking expectations in (6) and then interchanging expectation and contour integration (the justification of which is tedious but doable), we get

$$(7) \quad \mathbf{E}\nu_n(\Omega) = \frac{1}{2\pi i} \int_{\partial\Omega} \mathbf{E} \frac{P'_n(z)}{P_n(z)} dz.$$

The following Lemma shows that, away from the set $\{z \mid D_0(z) = 0\}$, the function

$$(8) \quad F(z) = \mathbf{E} \frac{P'_n(z)}{P_n(z)}$$

simplifies to the expression given in (5) and, since we've assumed that $\partial\Omega$ intersects this set at only finitely many points, this finishes the proof. \square

LEMMA 2.2. *Let F denote the function defined by (8). For $z \notin \{z \mid D_0(z) = 0\}$,*

$$F = \frac{B_1 D_0 + B_0 B_1 - \bar{A}_0 A_1}{B_0 D_0 + B_0^2 - \bar{A}_0 A_0}.$$

PROOF. Note that $P_n(z)$ and $P'_n(z)$ are complex Gaussian random variables. It is convenient to work with their real and imaginary parts,

$$\begin{aligned} P_n(z) &= \xi_1 + i\xi_2, \\ P'_n(z) &= \xi_3 + i\xi_4, \end{aligned}$$

which are just linear combinations of the original standard normal random variables:

$$\begin{aligned} \xi_1 &= \sum_{j=0}^n a_j \eta_j, & \xi_2 &= \sum_{j=0}^n b_j \eta_j, \\ \xi_3 &= \sum_{j=0}^n c_j \eta_j, & \xi_4 &= \sum_{j=0}^n d_j \eta_j. \end{aligned}$$

The coefficients in these linear combinations are given by

$$(9) \quad \begin{aligned} a_j &= \operatorname{Re}(f_j(z)) = \frac{f_j(z) + \overline{f_j(z)}}{2}, \\ b_j &= \operatorname{Im}(f_j(z)) = \frac{f_j(z) - \overline{f_j(z)}}{2i}, \\ c_j &= \operatorname{Re}(f'_j(z)) = \frac{f'_j(z) + \overline{f'_j(z)}}{2}, \\ d_j &= \operatorname{Im}(f'_j(z)) = \frac{f'_j(z) - \overline{f'_j(z)}}{2i}. \end{aligned}$$

Put $\xi = [\xi_1 \ \xi_2 \ \xi_3 \ \xi_4]^T$. The covariance among these four Gaussian random variables is easy to compute:

$$(10) \quad \text{Cov}(\xi) = \mathbf{E}\xi\xi^T = \begin{bmatrix} a^T a & a^T b & a^T c & a^T d \\ b^T a & b^T b & b^T c & b^T d \\ c^T a & c^T b & c^T c & c^T d \\ d^T a & d^T b & d^T c & d^T d \end{bmatrix}$$

We now represent these four correlated Gaussian random variables in terms of four independent standard normals. To this end, we seek a lower triangular matrix $L = [l_{ij}]$ such that the vector ξ is equal in distribution to $L\zeta$, where $\zeta = [\zeta_1 \ \zeta_2 \ \zeta_3 \ \zeta_4]^T$ is a vector of four independent standard normal random variables. The following simple calculation shows that L is the Cholesky factor for the covariance matrix:

$$(11) \quad \text{Cov}(\xi) = \mathbf{E}\xi\xi^T = \mathbf{E}L\zeta\zeta^T L^T = LL^T.$$

Now, since $\xi \stackrel{\text{D}}{=} L\zeta$ and L is lower triangular (the symbol $\stackrel{\text{D}}{=}$ denotes equality in distribution), we get that

$$\begin{aligned} \frac{P'_n(z)}{P_n(z)} &= \frac{\xi_3 + i\xi_4}{\xi_1 + i\xi_2} \\ &\stackrel{\text{D}}{=} \frac{(l_{31} + il_{41})\zeta_1 + (l_{32} + il_{42})\zeta_2 + (l_{33} + il_{43})\zeta_3 + il_{44}\zeta_4}{(l_{11} + il_{21})\zeta_1 + il_{22}\zeta_2}. \end{aligned}$$

Hence, exploiting the independence of the ζ_i 's, we see that

$$(12) \quad F(z) = \mathbf{E} \frac{P'_n(z)}{P_n(z)} = \mathbf{E} \frac{\alpha\zeta_1 + \beta\zeta_2}{\gamma\zeta_1 + \delta\zeta_2},$$

where

$$\begin{aligned} \alpha &= l_{31} + il_{41} & \beta &= l_{32} + il_{42} \\ \gamma &= l_{11} + il_{21} & \delta &= il_{22}. \end{aligned}$$

Splitting up the numerator in (12) and exploiting the exchangeability of ζ_1 and ζ_2 , we can rewrite the expectation as follows:

$$F(z) = \frac{\alpha}{\delta} f(\gamma/\delta) + \frac{\beta}{\gamma} f(\delta/\gamma),$$

where f is a complex-valued function defined on $\mathbf{C} \setminus \mathbf{R}$ by

$$f(w) = \mathbf{E} \frac{\zeta_1}{w\zeta_1 + \zeta_2}.$$

The expectation appearing in the definition of f can be explicitly computed. Indeed,

$$\begin{aligned} f(w) &= \frac{1}{2\pi} \int_0^{2\pi} \int_0^\infty \frac{\rho \cos \theta}{w \rho \cos \theta + \rho \sin \theta} e^{-\rho^2/2} \rho d\rho d\theta \\ &= \frac{1}{2\pi} \int_0^{2\pi} \frac{d\theta}{w + \tan \theta} \end{aligned}$$

and this last integral can be computed explicitly giving us

$$f(w) = \begin{cases} \frac{1}{w+i}, & \text{Im}(w) > 0, \\ \frac{1}{w-i}, & \text{Im}(w) < 0. \end{cases}$$

Recalling the definition of δ and γ , we see that

$$\frac{\gamma}{\delta} = \frac{l_{21}}{l_{22}} - i \frac{l_{11}}{l_{22}}.$$

In general, l_{11} and l_{22} are just nonnegative. However, it is not hard to show that they are both strictly positive whenever z has a nonzero imaginary part. Hence, γ/δ lies in the lower half-plane, δ/γ lies in the upper half-plane, and

$$\begin{aligned} (13) \quad F(z) &= \frac{\alpha}{\delta} \frac{1}{\frac{\gamma}{\delta} - i} + \frac{\beta}{\gamma} \frac{1}{\frac{\delta}{\gamma} + i} \\ &= \frac{i\alpha + \beta}{i\gamma + \delta} \\ &= \frac{l_{32} - l_{41} + i(l_{31} + l_{42})}{-l_{21} + i(l_{11} + l_{22})}. \end{aligned}$$

At this point, we need explicit formulas for the elements of the Cholesky factor L . From (10) and (11), we see that

$$\begin{aligned} a^T a &= l_{11}^2 \\ b^T a &= l_{21} l_{11} & b^T b &= l_{21}^2 + l_{22}^2 \\ c^T a &= l_{31} l_{11} & c^T b &= l_{31} l_{21} + l_{32} l_{22} \\ d^T a &= l_{41} l_{11} & d^T b &= l_{41} l_{21} + l_{42} l_{22}. \end{aligned}$$

Solving these equations in succession, we get

$$\begin{aligned}
l_{11} &= \frac{a^T a}{\sqrt{a^T a}} \\
l_{21} &= \frac{b^T a}{\sqrt{a^T a}} & l_{22} &= \frac{(a^T a)(b^T b) - (b^T a)^2}{\sqrt{a^T a} R} \\
l_{31} &= \frac{c^T a}{\sqrt{a^T a}} & l_{32} &= \frac{(a^T a)(c^T b) - (c^T a)(b^T a)}{\sqrt{a^T a} R} \\
l_{41} &= \frac{d^T a}{\sqrt{a^T a}} & l_{42} &= \frac{(a^T a)(d^T b) - (d^T a)(b^T a)}{\sqrt{a^T a} R}
\end{aligned}$$

where

$$R = \sqrt{(a^T a)(b^T b) - (b^T a)^2}.$$

Substituting these expressions into (13) and simplifying, we see that

$$(14) \quad F(z) = \frac{-d^T a + ic^T a - i(a^T a(-d^T b + ic^T b) - (-d^T a + ic^T a)b^T a) / R}{-b^T a + ia^T a + iR}.$$

Recalling the definitions of a_j , b_j , c_j , and d_j given in (9), it is easy to check that the following identities hold:

$$\begin{aligned}
a^T a &= \frac{1}{4}(A_0 + 2B_0 + \bar{A}_0), \\
b^T a &= -\frac{i}{4}(A_0 - \bar{A}_0), & b^T b &= -\frac{1}{4}(A_0 - 2B_0 + \bar{A}_0), \\
c^T a &= \frac{1}{4}(A_1 + B_1 + \bar{B}_1 + \bar{A}_1), & c^T b &= -\frac{i}{4}(A_1 - B_1 + \bar{B}_1 - \bar{A}_1), \\
d^T a &= -\frac{i}{4}(A_1 + B_1 - \bar{B}_1 - \bar{A}_1), & d^T b &= -\frac{1}{4}(A_1 - B_1 - \bar{B}_1 + \bar{A}_1).
\end{aligned}$$

Plugging these expressions into (14) and simplifying, we get that

$$(15) \quad F(z) = \frac{A_1 + B_1 + (A_0 B_1 + B_0 B_1 - A_1 B_0 - \bar{A}_0 A_1) / D_0}{A_0 + B_0 + D_0},$$

where D_0 is as given in (1). It turns out that further simplification occurs if we make the denominator real by the usual technique of multiplying and dividing by its complex conjugate. We leave out the algebraic details except to mention that a factor of $A_0 + 2B_0 + \bar{A}_0$ cancels out from the numerator and denominator leaving us with

$$(16) \quad F(z) = \frac{B_1 D_0 + B_0 B_1 - \bar{A}_0 A_1}{D_0(B_0 + D_0)},$$

or, expanding out D_0^2 ,

$$(17) \quad F(z) = \frac{B_1 D_0 + B_0 B_1 - \bar{A}_0 A_1}{B_0 D_0 + B_0^2 - \bar{A}_0 A_0}.$$

□

LEMMA 2.3. *On the real axis, F has a jump discontinuity. Indeed, for each $a \in \mathbb{R}$,*

$$\lim_{z \rightarrow a: \operatorname{Im}(z) > 0} F = \frac{B_1(a) - i E_1(a)}{B_0(a)}$$

and

$$\lim_{z \rightarrow a: \operatorname{Im}(z) < 0} F = \frac{B_1(a) + i E_1(a)}{B_0(a)}.$$

PROOF. Consider a point a on the real axis. On the reals, $A_k = B_k$, for $k = 0, 1$, and so $D_0 = 0$. Hence, the right-hand side in (16) is an indeterminate form. To analyze the limiting behavior of F near the real axis, we first divide the numerator and denominator by D_0 :

$$(18) \quad F = \frac{B_1 + \frac{B_0 B_1 - \bar{A}_0 A_1}{D_0}}{B_0 + D_0}.$$

Now, only the ratio in the numerator is indeterminate. To study it, we start by expressing things in terms of the f_j functions:

$$\begin{aligned} B_0 B_1 - \bar{A}_0 A_1 &= \sum_{j,k} \overline{f_j(z)} f'_k(z) \left(f_j(z) \overline{f_k(z)} - \overline{f_j(z)} f_k(z) \right) \\ &= 2i \sum_{j,k} \overline{f_j(z)} f'_k(z) \operatorname{Im} \left(f_j(z) \overline{f_k(z)} \right) \end{aligned}$$

and

$$\begin{aligned} D_0^2 &= B_0^2 - |A_0|^2 = \sum_{j,k} f_j(z) \overline{f_k(z)} \left(\overline{f_j(z)} f_k(z) - f_j(z) \overline{f_k(z)} \right) \\ &= -2i \sum_{j,k} f_j(z) \overline{f_k(z)} \operatorname{Im} \left(f_j(z) \overline{f_k(z)} \right). \end{aligned}$$

Next, we write the first few terms of the Taylor series expansion of the f_j 's about the point $z = a$, substitute the expansions into the formulas above and then drop "high" order terms to derive the first few terms of the Taylor

expansions for $B_0B_1 - \bar{A}_0A_1$ and $B_0^2 - |A_0|^2$. For the first expression, we only need to go to linear terms to get

$$\begin{aligned} B_0B_1 - \bar{A}_0A_1 &= 2i \sum_{j,k} f_j(a)f'_k(a) \left(f'_j(a)f_k(a) - f_j(a)f'_k(a) \right) y + o(z-a) \\ &= 2i \left(A_1(a)^2 - A_0(a)A_2(a) \right) y + o(z-a) \end{aligned}$$

(as usual, we use y to denote the imaginary part of z). For the second expression, we need to go to quadratic terms. The result is

$$\begin{aligned} D_0^2 &= 4 \sum_{j,k} \left(f'_j(a)^2 f_k(a)^2 - f_j(a)f'_j(a)f_k(a)f'_k(a) \right) y^2 + o((z-a)^2) \\ &= 4 \left(\left(\sum_{j=0}^n f'_j(a)^2 \right) \left(\sum_{j=0}^n f_j(a)^2 \right) - \left(\sum_{j=0}^n f'_j(a)f_j(a) \right)^2 \right) y^2 + o((z-a)^2) \\ &= 4 \left(A_2(a)A_0(a) - A_1(a)^2 \right) y^2 + o((z-a)^2). \end{aligned}$$

Hence, we see that

$$(19) \quad \frac{B_0B_1 - \bar{A}_0A_1}{D_0} = -i E_1(a) \operatorname{sgn}(a) \operatorname{sgn}(y) + o(z-a).$$

Combining (18) and (19), we get the desired limits expressing the jump discontinuity on the real axis. \square

Proof of Theorem 1.1.. Without loss of generality, it suffices to consider regions Ω that are either regions that do not intersect the real axis or small rectangles centered on the real axis. We begin by considering a region Ω that does not intersect the real axis. Applying Stokes' theorem to the expression for $\mathbf{E}\nu_n(\Omega)$ given in Proposition 2.1, we see that

$$\mathbf{E}\nu_n(\Omega) = \frac{1}{\pi} \int_{\Omega} \frac{\partial}{\partial \bar{z}} F(z, \bar{z}) dx dy.$$

Note that we are now writing $F(z, \bar{z})$ to emphasize the fact that F depends on both z and \bar{z} . Letting the dagger symbol stand for the derivative with respect to \bar{z} , we see from Lemma 2.2 that

$$(20) \quad \begin{aligned} \frac{\partial F}{\partial \bar{z}} &= \left\{ (B_0D_0 + B_0^2 - \bar{A}_0A_0)(B_1^\dagger D_0 + B_1D_0^\dagger + B_0^\dagger B_1 + B_0B_1^\dagger - \bar{A}_0^\dagger A_1) \right. \\ &\quad \left. - (B_1D_0 + B_0B_1 - \bar{A}_0A_1)(B_0^\dagger D_0 + B_0D_0^\dagger + 2B_0B_0^\dagger - \bar{A}_0^\dagger A_0) \right\} \\ &\quad / (B_0D_0 + B_0^2 - |A_0|^2)^2. \end{aligned}$$

Recall that we have assumed that the functions f_j are entire and are real-valued on the real line. Hence, they have the property that $\overline{f_j(z)} = f_j(\bar{z})$. Their derivatives also have this property. Exploiting these facts, it is easy to check that

$$(21) \quad B_0^\dagger = \bar{B}_1, \quad \bar{A}_0^\dagger = 2\bar{A}_1, \quad B_1^\dagger = B_2.$$

Recalling that $D_0 = \sqrt{B_0^2 - |A_0|^2}$, we get that

$$(22) \quad D_0^\dagger = \frac{B_0\bar{B}_1 - A_0\bar{A}_1}{D_0}.$$

As explained in [22], substituting these formulas for the derivatives into the expression given above for $\partial F/\partial\bar{z}$ followed by careful algebraic simplifications (see the appendix for the details) eventually leads to the fact that $(1/\pi)\partial F(z, \bar{z})/\partial\bar{z}$ equals the expression given for h_n in the statement of the theorem. \square

Proof of Theorem 1.2.. Consider a narrow rectangle that straddles an interval of the real axis: $\Omega = [a, b] \times [-\varepsilon, \varepsilon]$ where $a < b$ and $\varepsilon > 0$. Writing the contour integral for $\mathbf{E}\nu_n(\Omega)$ given by Proposition 2.1 and letting ε tend to 0, we see that

$$\mathbf{E}\nu_n((a, b)) = \frac{1}{2\pi i} \int_a^b (F(x-) - F(x+)) dx,$$

where $\nu_n((a, b))$ denotes the number of zeros in the interval (a, b) of the real axis and

$$F(x-) = \lim_{z \rightarrow x: \text{Im}(z) < 0} F(z) \quad \text{and} \quad F(x+) = \lim_{z \rightarrow x: \text{Im}(z) > 0} F(z).$$

From Lemma 2.3, we see that

$$g_n(x) = \frac{1}{2\pi i} (F(x-) - F(x+)) = \frac{E_1(x)}{\pi B_0}.$$

This completes the proof. \square

3. Examples.. In this section, we consider some examples. The simplest example corresponds to the f_j simply being the power functions:

$$f_j(z) = z^j.$$

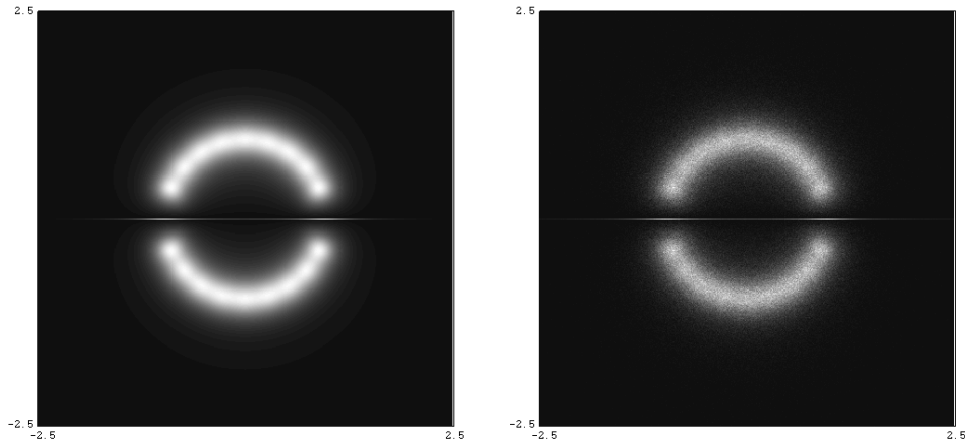


FIG 1. *Random degree 10 polynomial: $\eta_0 + \eta_1 z + \eta_2 z^2 + \dots + \eta_{10} z^{10}$. In this figure and the following ones, the left-hand plot is a grey-scale image of the intensity functions h_n and g_n (the latter being concentrated on the x-axis). The right-hand plot shows 200,000 roots from randomly generated polynomials. Note that, for the left-hand plots, the grey-scales for h_n and g_n are scaled separately and in such a way that both use the full range from white to black.*

As this case was studied carefully in [22], other than showing a particular example ($n = 10$) in Figure 1, we refer the reader to that previous paper for more information about this example.

Each figure in this section shows two plots. On the left is a grey-scale plot of the intensity functions g_n and h_n . On the right is a plot of hundreds of thousands of zeros obtained by generating random sums and explicitly finding their zeros.

The intensity plots appearing on the left were produced by partitioning the given square domain into a 440 by 440 grid of “pixels” and computing the intensity function in the center of each pixel. The grey-scale was computed by assigning black to the pixel with the smallest value and white to the pixel with the largest value and then linearly interpolating all values in between. This grey-scale computation was performed separately for h_n and for g_n (which appears only on the x-axis) and so no conclusions should be drawn comparing the intensity shown on the x-axis with that shown off from it. The applet used to produce these figures can be found at

<http://www.princeton.edu/~rvdb/JAVA/Roots/Roots.html>

Of course, the intensity function g_n is one-dimensional and therefore it would be natural (and more informative) to make separate plots of values

of g_n versus x , but such plots appear in many places (see, e.g., [16]) and so it seemed unnecessary to produce them here.

3.1. *Weyl Polynomials.* Sums in which the f_j 's are given by

$$f_j(z) = \frac{z^j}{\sqrt{j!}}$$

are called *Weyl polynomials* (also sometimes called *flat polynomials*). Figure 4 shows the empirical distribution for the case where $n = 10$. For this case, the limiting forms of the various functions defining the densities are easy to compute:

$$\begin{aligned} \lim_{n \rightarrow \infty} A_0(z) &= e^{z^2} & \lim_{n \rightarrow \infty} B_0(z) &= e^{|z|^2} \\ \lim_{n \rightarrow \infty} A_1(z) &= ze^{z^2} & \lim_{n \rightarrow \infty} B_1(z) &= \bar{z}e^{|z|^2} \\ \lim_{n \rightarrow \infty} A_2(z) &= (z^2 + 1)e^{z^2} & \lim_{n \rightarrow \infty} B_2(z) &= (|z|^2 + 1)e^{|z|^2} \\ \lim_{n \rightarrow \infty} D_0(z) &= \sqrt{e^{2(x^2+y^2)} - e^{4(x^2-y^2)}} & \lim_{n \rightarrow \infty} E_1(z) &= e^{z^2}. \end{aligned}$$

The random Weyl polynomials are interesting because in the limit as $n \rightarrow \infty$, the distribution of the real roots becomes uniform over the real line:

THEOREM 3.1. *If $f_j(z) = z^j/\sqrt{j!}$ for all j , then*

$$\lim_{n \rightarrow \infty} g_n(x) = \frac{1}{\pi}.$$

PROOF. Follows trivially from Theorem 1.2 and the formulas above. \square

It is interesting to note that, in addition to the asymptotic uniformity of the distribution of the real roots, the complex roots are also much more uniformly distributed than was the case when we did not have the $1/\sqrt{j!}$ factors.

Figure 3 shows plots of g_n for all of the examples considered here.

3.2. *Taylor Polynomials.* Another obvious set of polynomials to consider are the random Taylor polynomials; i.e., those polynomials with

$$f_j(z) = \frac{z^j}{j!}.$$

Figure 2 shows the $n = 10$ empirical distribution for these polynomials.

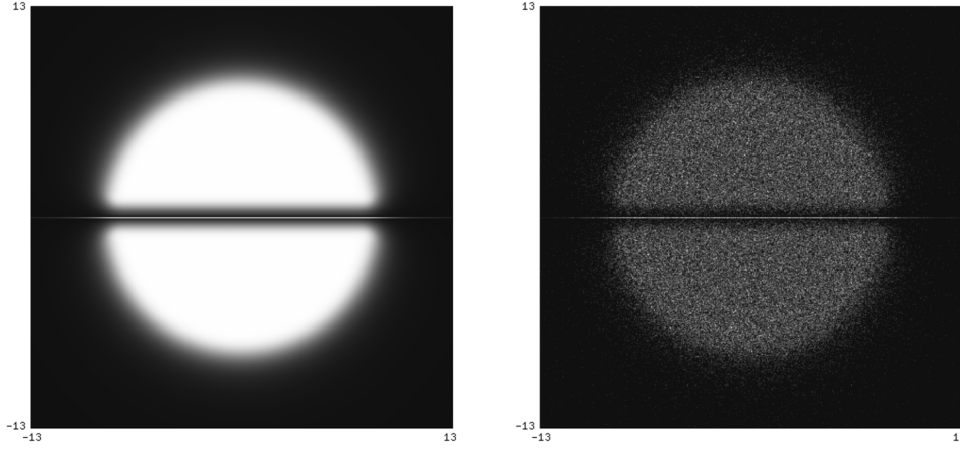


FIG 2. *Random degree 10 Weyl polynomials: $\eta_0 + \eta_1 z + \eta_2 \frac{z^2}{\sqrt{2!}} + \cdots + \eta_{80} \frac{z^{80}}{\sqrt{80!}}$. The empirical distribution on the right was generated using 2,500 random sums.*

3.3. *Root-Binomial Polynomials.* Let

$$f_j(z) = \sqrt{\binom{n}{j}} z^j.$$

Figure 5 shows the $n = 10$ empirical distribution for these polynomials. This example is interesting because the real and complex density functions take on a rather simple explicit form. Indeed, it is easy to check that

$$\begin{aligned} A_0(z) &= (1 + z^2)^n, & B_0(z) &= (1 + |z|^2)^n, \\ A_1(z) &= nz(1 + z^2)^{n-1}, & B_1(z) &= n\bar{z}(1 + |z|^2)^{n-1}, \\ A_2(z) &= n(1 + nz^2)(1 + z^2)^{n-2}, & B_2(z) &= n(1 + n|z|^2)(1 + |z|^2)^{n-2}. \end{aligned}$$

The formula for the density on the real axis simplifies nicely:

$$g(x) = \frac{\sqrt{n}}{\pi} \frac{1}{1 + x^2}.$$

From this formula, we see that the expected number of real roots is \sqrt{n} and that each real root has a Cauchy distribution.

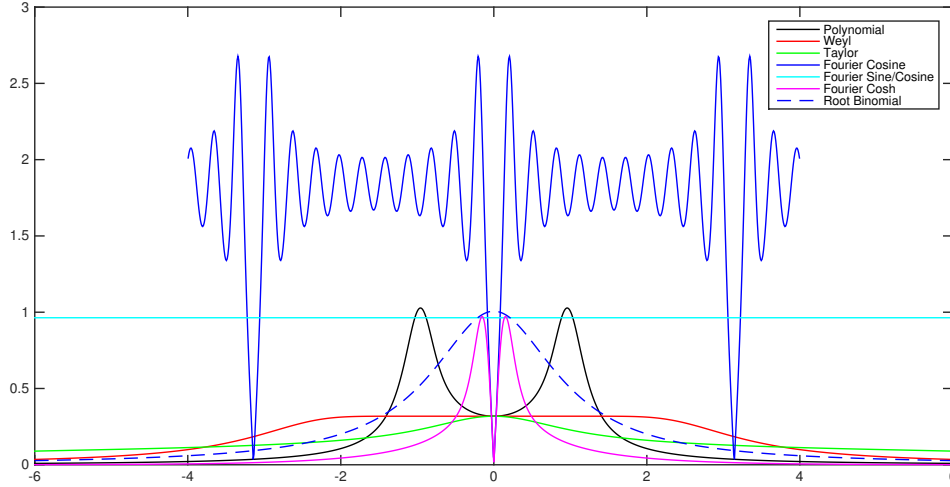


FIG 3. The function g_n for $n = 10$ for several choices of the f_j 's

3.4. *Fourier Cosine Series.* Now let's consider a family of random sums that are not polynomials, namely, random (truncated) Fourier cosine series:

$$f_j(z) = \cos(jz).$$

This case is interesting because these functions are real-valued not only on the real axis but on the imaginary axis as well: $\cos(iy) = \cosh(y)$. Hence, D_0 vanishes on both the real and the imaginary axes and, therefore, both axes have a density of zeros. The set of imaginary roots for a particular sum using the f_j 's map to a set of real roots if $f_j(z)$ is replaced with $\tilde{f}_j(z) = f_j(iz) = \cosh(z)$. Hence, the formula for the density on the imaginary axis is easy to compute by this simple rotation. The resulting density on the imaginary axis has this simple form:

$$g_n(y) = \frac{E_1(iy)}{\pi B_0(iy)}.$$

An example with $n = 10$ is shown in Figure 6.

3.5. *Fourier Sine/Cosine Series.* Finally, we consider random (truncated) Fourier sine/cosine series:

$$f_j(z) = \begin{cases} \cos(\frac{j}{2}z), & j \text{ even,} \\ \sin(\frac{j+1}{2}z), & j \text{ odd.} \end{cases}$$

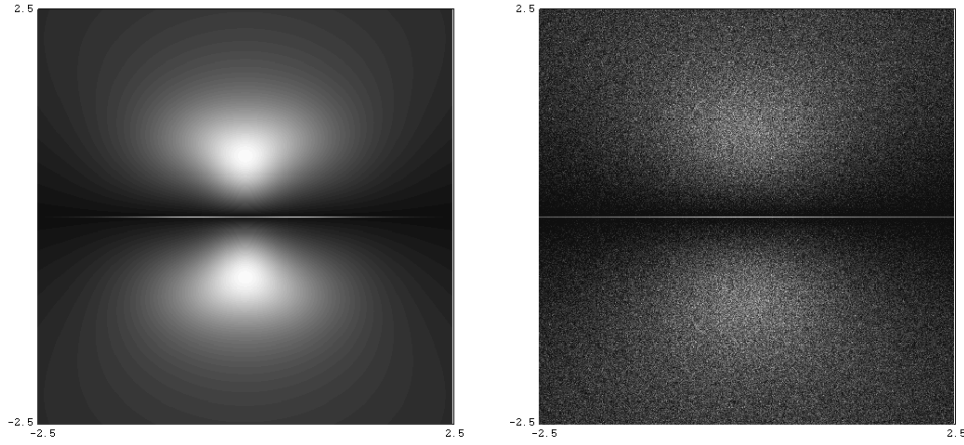


FIG 4. *Random degree 10 Taylor polynomials: $\eta_0 + \eta_1 z + \eta_2 \frac{z^2}{2!} + \dots + \eta_{10} \frac{z^{10}}{10!}$. The empirical distribution on the right was generated using 500,000 random sums.*

The $n = 2$ case is shown in Figure 7 and the $n = 10$ case is shown in Figure 8. For this example, it is easy to compute the key functions. Assuming that n is even and letting $m = n/2$, we get

$$\begin{aligned}
 A_0(z) &= m + 1 & B_0(z) &= m + 1 + 2 \sum_{j=1}^m \sinh^2(jy) \\
 A_1(z) &= 0 & B_1(z) &= -2i \sum_{j=1}^m j \cosh(jy) \sinh(jy) \\
 A_2(z) &= m(m+1)(2m+1)/6 & B_2(z) &= 2 \sum_{j=1}^m j^2 \sinh^2(jy)
 \end{aligned}$$

From these explicit formulas, it is easy to check that the density function $h_n(z)$ depends only on the imaginary part of z as is evident in Figures 7 and 8. It is also easy to check that the distribution on the real axis is uniform; i.e., the density function $g_n(x)$ is a constant:

$$g_n(x) = \frac{1}{2\pi} \sqrt{n(n+1)/3}.$$

4. Final Comments and Suggested Future Research.. The machinery developed in this paper can be applied in many situations that we have not covered. For example, if the coefficients are assumed to be independent complex Gaussians (instead of real), then we can apply the same methods and we expect that the computations will be simpler. In this case,

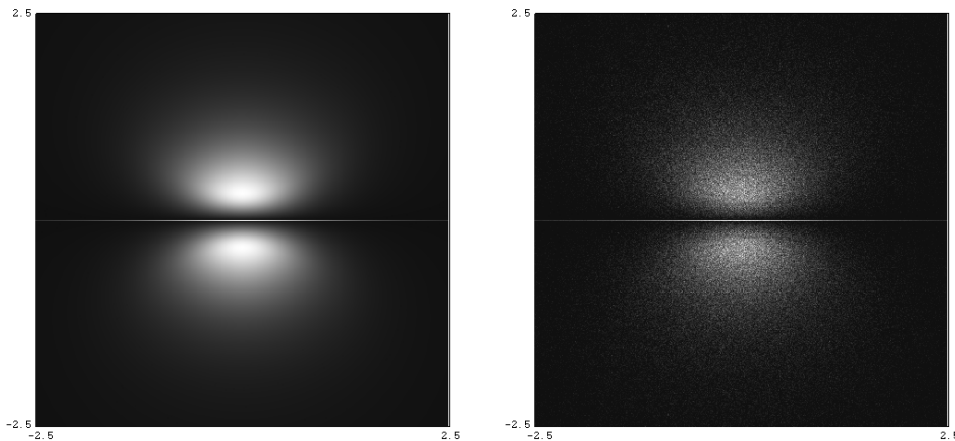


FIG 5. *Random degree 10 root-binomial polynomials: $\eta_0 + \eta_1 \sqrt{\frac{10}{1}}z + \eta_2 \sqrt{\frac{10 \cdot 9}{2 \cdot 1}}z^2 + \eta_3 \sqrt{\frac{10 \cdot 9 \cdot 8}{3 \cdot 2 \cdot 1}}z^3 + \dots + \eta_{10}z^{10}$. The empirical distribution on the right was generated using 50,000 random sums.*

the intensity function does not have mass concentrated on the real axis (i.e., $g_n = 0$) and the intensity function is rotationally invariant.

Acknowledgement. The author would like to thank John P. D'Angelo for helpful comments.

REFERENCES

- [1] AHLFORS, L. V. (1966). *Complex Analysis*. McGraw-Hill, New York.
- [2] BHARUCHA-REID, A. T. and SAMBANDHAM, M. (1986). *Random Polynomials*. Academic Press.
- [3] DEMBO, A., POONEN, B., SHAO, Q.-M. and ZEITOUNI, O. (2002). Random polynomials having few or no real zeros. *Journal of the American Mathematical Society* **15** 857–892.
- [4] EDELMAN, A. and KOSTLAN, E. (1995). How many zeros of a random polynomial are real? *Bulletin of the American Mathematical Society* **32** 1–37.
- [5] ERDÖS, P. and TURÁN, P. (1950). On the distribution of roots of polynomials. *Ann. Math.* **51** 105–119.
- [6] FELDHEIM, N. D. (2012). Zeros of Gaussian Analytic Functions with Translation-Invariant Distribution. *Israel J. of Math.* **195** 317–345.
- [7] FORRESTER, P. and HONNER, G. (1999). Exact statistical properties of the zeros of complex random polynomials. *Journal of Physics A: Mathematical and General* **32** 2961.
- [8] HAMMERSLEY, J. (1956). The zeros of a random polynomial. In *Proc. Third Berkeley Symp. Math. Stat. Probability* **2** 89–111.

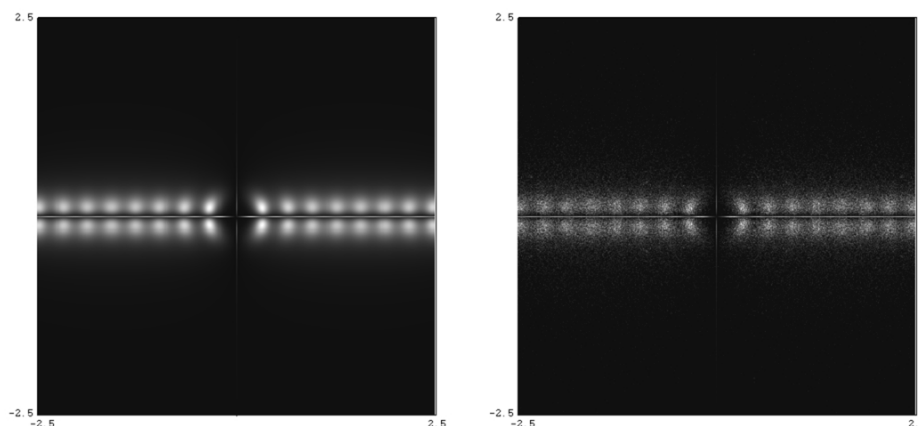


FIG 6. *Random sum of first 11 terms in a cosine Fourier series: $\eta_0 + \eta_1 \cos(z) + \eta_2 \cos(2z) + \dots + \eta_{10} \cos(10z)$. The empirical distribution on the right was generated using 24,000 random sums.*

- [9] HUGHES, C. P. and NIKEGHBALI, A. (2008). The zeros of random polynomials cluster uniformly near the unit circle. *Compositio Mathematica* **144** 734–746.
- [10] IBRAGIMOV, I. and ZAPOROZHETS, D. (2013). On distribution of zeros of random polynomials in complex plane. In *Prokhorov and contemporary probability theory* 303–323. Springer.
- [11] IBRAGIMOV, I. and ZEITOUNI, O. (1997). On roots of random polynomials. *Transactions of the American Mathematical Society* **349** 2427–2441.
- [12] JR., J. E. W. (1997). The Expected Value of the Number of Real Zeros of a Random Sum of Legendre Polynomials. *Proc. Amer. Math. Soc.* **125** 1531–1536.
- [13] KABLUCHKO, Z. and ZAPOROZHETS, D. (13). Roots of Random Polynomials whose Coefficients Have Logarithmic Tails. *Ann. Prob.* **41** 3542–3581.
- [14] KABLUCHKO, Z. and ZAPOROZHETS, D. (14). Asymptotic Distribution of Complex Zeros of Random Analytic Functions. *Ann. Prob.* **42** 1374–1395.
- [15] KAC, M. (1943). On the average number of real roots of a random algebraic equation. *Bull. Amer. Math. Soc.* **49** 314–320,938.
- [16] KAC, M. (1959). *Probability and related topics in physical sciences*. Interscience, London.
- [17] LI, W. and WEI, A. (2009). On the expected number of zeros of a random harmonic polynomial. *Proceedings of the American Mathematical Society* **137** 195–204.
- [18] PRITSKER, I. E. (2017). Zero Distribution of Random Polynomials. *J. Anal. Math.* To appear.
- [19] PRITSKER, I. E. and YEAGER, M. A. (2015). Zeros of Polynomials with Random Coefficients. *J. Approx. Theory* **189** 88–100.
- [20] PROSEN, T. (1996). Exact statistics of complex zeros for Gaussian random polynomials with real coefficients. *Journal of Physics A: Mathematical and General* **29** 4417.

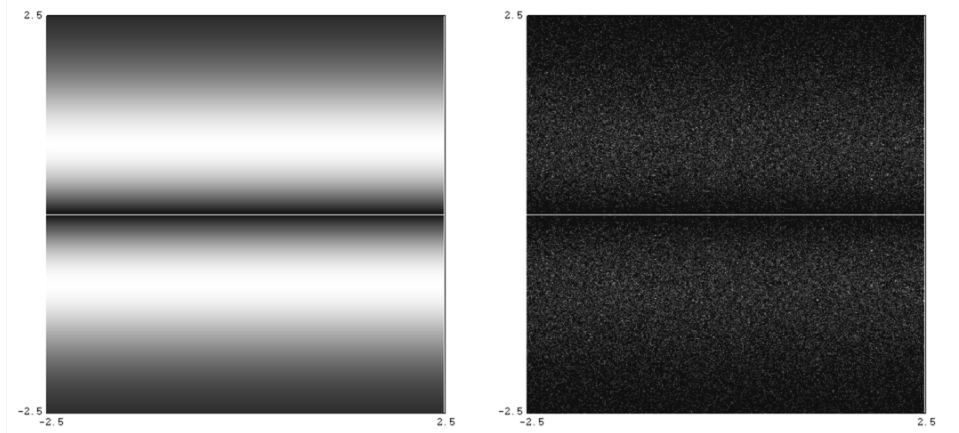


FIG 7. Random sum of first 3 terms in a sine/cosine Fourier series: $\eta_0 + \eta_1 \sin(z) + \eta_2 \cos(z)$. The empirical distribution on the right was generated using 210,000 random sums.

- [21] SCHEHR, G. and MAJUMDAR, S. N. (2009). Condensation of the Roots of Real Random Polynomials on the Real Axis. *J. Stat. Physics* **135** 587–598.
- [22] SHEPP, L. A. and VANDERBEI, R. J. (1995). The complex zeros of random polynomials. *Transactions of the AMS* **347** 4365–4384.
- [23] SHIFFMAN, B. and ZELDITCH, S. (2003). Equilibrium distribution of zeros of random polynomials. *International Mathematics Research Notices* **2003** 25–49.
- [24] TAO, T. and VU, V. (2014). Local universality of zeroes of random polynomials. *International Mathematics Research Notices* 1–84.
- [25] ŠPARO, D. I. and ŠUR, M. G. (1962). On the distribution of roots of random polynomials. *Vestn. Mosk. Univ., Ser. 1: Mat., Mekh.* 40–53.

APPENDIX A: ALGEBRAIC SIMPLIFICATION OF THE FORMULA FOR $\partial F/\partial \bar{z}$.

Substituting the derivatives given in (21) and (22) into the formula (20) for $\partial F/\partial \bar{z}$, we get that the denominator simplifies to

$$\begin{aligned}
 \text{denom} \left(\frac{\partial F}{\partial \bar{z}} \right) &= \left(B_0 D_0 + B_0^2 - \bar{A}_0 A_0 \right)^2 \\
 &= \left(B_0 D_0 + D_0^2 \right)^2 \\
 &= (B_0 + D_0)^2 D_0^2.
 \end{aligned}$$

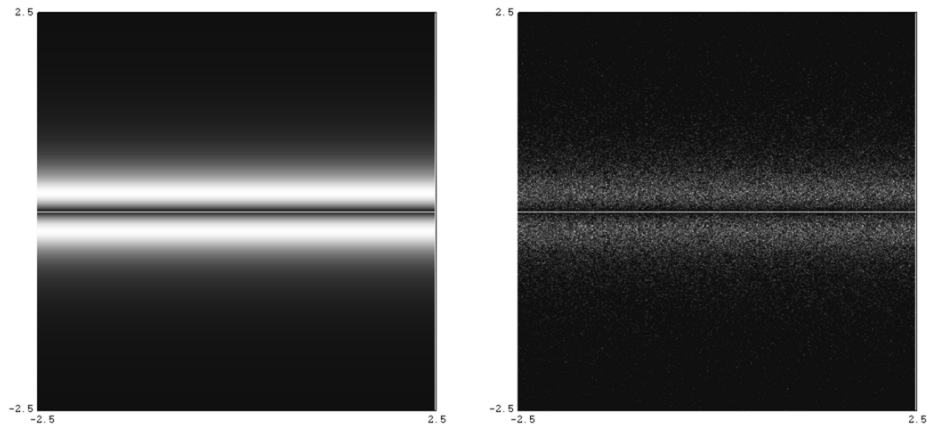


FIG 8. *Random sum of first 11 terms in a sine/cosine Fourier series: $\eta_0 + \eta_1 \sin(z) + \eta_2 \cos(z) + \dots + \eta_9 \sin(5z) + \eta_{10} \cos(5z)$. The empirical distribution on the right was generated using 26,000 random sums.*

and the numerator of the formula becomes

$$\begin{aligned} \text{num} \left(\frac{\partial F}{\partial \bar{z}} \right) &= (B_0 D_0 + B_0^2 - \bar{A}_0 A_0) \left(B_2 D_0 + B_1 \frac{B_0 \bar{B}_1 - A_0 \bar{A}_1}{D_0} \right. \\ &\quad \left. + \bar{B}_1 B_1 + B_0 B_2 - 2 \bar{A}_1 A_1 \right) \\ &\quad - (B_1 D_0 + B_0 B_1 - \bar{A}_0 A_1) \left(\bar{B}_1 D_0 + B_0 \frac{B_0 \bar{B}_1 - A_0 \bar{A}_1}{D_0} \right. \\ &\quad \left. + 2 B_0 \bar{B}_1 - 2 \bar{A}_1 A_0 \right). \end{aligned}$$

The first step to simplifying the numerator is to replace $B_0^2 - \bar{A}_0 A_0$ in the first term with D_0 (like we did in the denominator) and factor out a $1/D_0$ to get

$$\begin{aligned} \text{num} \left(\frac{\partial F}{\partial \bar{z}} \right) &= \frac{1}{D_0} (B_0 + D_0) D_0 \left(B_2 D_0^2 + B_1 B_0 \bar{B}_1 - B_1 A_0 \bar{A}_1 \right. \\ &\quad \left. + \bar{B}_1 B_1 D_0 + B_0 B_2 D_0 - 2 \bar{A}_1 A_1 D_0 \right) \\ &\quad - \frac{1}{D_0} ((B_0 + D_0) B_1 - \bar{A}_0 A_1) \left(\bar{B}_1 D_0^2 + B_0 B_0 \bar{B}_1 - B_1 A_0 \bar{A}_1 \right. \\ &\quad \left. + 2 B_0 \bar{B}_1 D_0 - 2 \bar{A}_1 A_0 D_0 \right). \end{aligned}$$

Next, we bundle together the terms that have a $B_0 + D_0$ factor:

$$\begin{aligned} \text{num} \left(\frac{\partial F}{\partial \bar{z}} \right) &= \frac{1}{D_0} (B_0 + D_0) \left(B_2 D_0^3 + B_1 B_0 \bar{B}_1 D_0 - B_1 A_0 \bar{A}_1 D_0 \right. \\ &\quad \left. + \bar{B}_1 B_1 D_0^2 + B_0 B_2 D_0^2 - 2 \bar{A}_1 A_1 D_0^2 \right. \\ &\quad \left. - |B_1|^2 D_0^2 - B_0 B_0 |B_1|^2 + B_1^2 A_0 \bar{A}_1 \right. \\ &\quad \left. - 2 B_0 |B_1|^2 D_0 + 2 \bar{A}_1 A_0 B_1 D_0 \right) \\ &\quad + \frac{1}{D_0} \bar{A}_0 A_1 \left(\bar{B}_1 D_0^2 + B_0 B_0 \bar{B}_1 - B_1 A_0 \bar{A}_1 \right. \\ &\quad \left. + 2 B_0 \bar{B}_1 D_0 - 2 \bar{A}_1 A_0 D_0 \right). \end{aligned}$$

Now, there are several places where we can find $B_0 + D_0$ factors. For example, the big factor containing eleven terms can be rewritten as follows:

$$\begin{aligned} &B_2 D_0^3 + B_1 B_0 \bar{B}_1 D_0 - B_1 A_0 \bar{A}_1 D_0 + \bar{B}_1 B_1 D_0^2 + B_0 B_2 D_0^2 - 2 \bar{A}_1 A_1 D_0^2 \\ &- |B_1|^2 D_0^2 - B_0 B_0 |B_1|^2 + B_1^2 A_0 \bar{A}_1 - 2 B_0 |B_1|^2 D_0 + 2 \bar{A}_1 A_0 B_1 D_0 \\ &= (B_0 + D_0) (B_2 D_0^2 - B_0 |B_1|^2 + A_0 \bar{A}_1 B_1) - 2 |A_1|^2 D_0^2. \end{aligned}$$

We also look for $B_0 + D_0$ factors in the five-term factor:

$$\begin{aligned} &\bar{B}_1 D_0^2 + B_0 B_0 \bar{B}_1 - B_1 A_0 \bar{A}_1 + 2 B_0 \bar{B}_1 D_0 - 2 \bar{A}_1 A_0 D_0 \\ &= (B_0 + D_0) ((B_0 + D_0) \bar{B}_1 - A_0 \bar{A}_1) - A_0 \bar{A}_1 D_0. \end{aligned}$$

Substituting these expressions into the formula for the numerator, we get

$$\begin{aligned} D_0 \text{num} \left(\frac{\partial F}{\partial \bar{z}} \right) &= (B_0 + D_0) \left((B_0 + D_0) (B_2 D_0^2 - B_0 |B_1|^2 + A_0 \bar{A}_1 B_1) - 2 |A_1|^2 D_0^2 \right) \\ &\quad + \bar{A}_0 A_1 \left((B_0 + D_0) ((B_0 + D_0) \bar{B}_1 - A_0 \bar{A}_1) - A_0 \bar{A}_1 D_0 \right). \end{aligned}$$

Rearranging the terms, we see that

$$\begin{aligned} D_0 \text{num} \left(\frac{\partial F}{\partial \bar{z}} \right) &= (B_0 + D_0)^2 (B_2 D_0^2 - B_0 |B_1|^2 + A_0 \bar{A}_1 B_1 + \bar{A}_0 A_1 \bar{B}_1) \\ &\quad - (B_0 + D_0) \left(2 |A_1|^2 D_0^2 + |A_0|^2 |A_1|^2 \right) \\ &\quad - |A_0|^2 |A_1|^2 D_0. \end{aligned}$$

Here's the tricky part... replace D_0^2 in the second row with $B_0^2 - |A_0|^2$ and the second and third row simplify nicely:

$$\begin{aligned}
& (B_0 + D_0) \left(2|A_1|^2 D_0^2 + |A_0|^2 |A_1|^2 \right) + |A_0|^2 |A_1|^2 D_0 \\
&= (B_0 + D_0) \left(2|A_1|^2 B_0^2 - |A_0|^2 |A_1|^2 \right) + |A_0|^2 |A_1|^2 D_0 \\
&= 2|A_1|^2 B_0^3 - |A_0|^2 |A_1|^2 B_0 + 2|A_1|^2 B_0^2 D_0 \\
&= |A_1|^2 B_0 \left(2B_0^2 - |A_0|^2 + 2B_0 D_0 \right) \\
&= |A_1|^2 B_0 (B_0 + D_0)^2.
\end{aligned}$$

Substituting this expression into our formula for the numerator, we now have

$$D_0 \operatorname{num} \left(\frac{\partial F}{\partial \bar{z}} \right) = (B_0 + D_0)^2 (B_2 D_0^2 - B_0 (|A_1|^2 + |B_1|^2) + A_0 \bar{A}_1 B_1 + \bar{A}_0 A_1 \bar{B}_1).$$

Finally, we get a simple formula for $\partial F / \partial \bar{z}$:

$$\frac{\partial F}{\partial \bar{z}} = \frac{B_2 D_0^2 - B_0 (|A_1|^2 + |B_1|^2) + A_0 \bar{A}_1 B_1 + \bar{A}_0 A_1 \bar{B}_1}{D_0^3}.$$

DEPT. OF OPS. RES. AND FIN. ENG.
PRINCETON UNIVERSITY
PRINCETON, NJ 08544